

# Disordered Josephson Junctions of $d$ -Wave Superconductors

Thomas Lück,\* Peter Schwab, and Ulrich Eckern

*Institut für Physik, Universität Augsburg, D-86135 Augsburg, Germany*

A. Shelankov

*Department of Theoretical Physics, Umeå University, 901 87, Sweden* <sup>†</sup>

(Dated: February 27, 2019)

We study the Josephson effect between weakly coupled  $d$ -wave superconductors within the quasiclassical theory, in particular, the influence of interface roughness on the current-phase relation and the critical current of mirror junctions and  $45^\circ$  asymmetric junctions. For mirror junctions the temperature dependence of the critical current is non-monotonic in the limit of low roughness, but monotonic for very rough interfaces. For  $45^\circ$  asymmetric junctions with a linear dimension much larger than the superconducting coherence length we find a  $\sin(2\varphi)$ -like current-phase relation, whereas for contacts on the scale of the coherence length or smaller the usual  $\sin\varphi$ -like behavior is observed. Our results compare well with recent experimental observations.

PACS numbers: 74.76.Bz, 74.50.+r

## I. INTRODUCTION

It is commonly believed that high- $T_c$  superconductors are described by an order parameter which dominantly exhibits  $d$ -wave symmetry. This was especially established by SQUID-like experiments, e.g. the corner-SQUID experiments by Wollmann et al.<sup>1</sup> or the tricrystal experiment by Tsuei et al.<sup>2</sup>, which provide a phase-sensitive test of the order parameter. This observation was followed by numerous theoretical studies of the Josephson effect between  $d$ -wave superconductors with rather unexpected results; a review can be found in Refs.<sup>3,4,5</sup>.

For instance a mirror junction, where the order parameter on the left and right hand side is rotated by the same angle but in opposite directions, should exhibit a non-monotonic temperature dependence of the critical current<sup>3,6,7</sup>; this behavior is related to a transition to a  $\pi$ -junction state at low temperatures. For the  $45^\circ$  asymmetric junction, in which the order parameter is rotated only on one side by  $45^\circ$ , a  $\sin(2\varphi)$ -like current-phase relation was predicted<sup>3</sup>, as the leading contribution to the tunnel current vanishes due to symmetry. Experimentally, the temperature dependence of the critical current<sup>8,9,10</sup> and the current-phase relation<sup>11,12,13</sup> of artificially produced grain boundaries with a well defined lattice orientation were determined. For mirror junctions the predicted non-monotonic behavior of the temperature-dependent critical current was found by Il'ichev et al.<sup>13</sup>, whereas in other cases a monotonic behavior as in usual  $s$ -wave superconductors was reported<sup>8,9,10</sup>. In the experiment on an asymmetric junction<sup>12</sup> not all samples showed the predicted  $\sin(2\varphi)$ -like current-phase relation.

As the  $d$ -wave order parameter is sensitive to disorder scattering it is believed that the origin for these differing results is interface roughness: One possibility is the existence of facets with spatially varying orientation which occur at the interfaces on a  $\mu\text{m}$ -scale<sup>14,15</sup>. This kind of

disorder can theoretically be described by a model consisting of randomly oriented mirrors<sup>16,17</sup>. On the other hand roughness on the atomic scale is present as well. In theoretical studies this is a non-trivial problem which we will tackle in this work. In previous studies interface roughness was modeled by a thin dirty layer next to a specular interface<sup>6,18,19</sup>. We use an alternative approach which allows us to study, at least in principle, also individual realizations of the disorder; this might be of importance for mesoscopically small junctions.

For the calculations we will use the quasiclassical theory of superconductivity<sup>20,21</sup> which is valid for spatial variations on scales which are large compared to the Fermi wave length,  $\lambda_F$ ; this is marginally fulfilled in the  $\text{CuO}_2$ -planes of high- $T_c$  materials as  $\xi_0/\lambda_F \approx 5$  ( $\xi_0$ : superconducting coherence length at zero temperature in the  $\text{CuO}_2$ -planes). Near interfaces the quasiclassical theory must be supplemented by boundary conditions. A specular interface can be described by Zaitsev's<sup>22</sup> boundary conditions. We use a more general scheme as suggested by Shelankov and Ozana<sup>23</sup>; this approach is extended in order to find suitable boundary conditions for interfaces. The properties of the interface, e.g. roughness or transparency, are incorporated by a scattering matrix. To describe an interface without regular structure we phenomenologically choose random scattering matrices. A similar approach has already been successfully applied to examine tunnel junctions between a normal metal and a  $d$ -wave superconductor<sup>24,25</sup>.

The paper is arranged as follows: In the next section we briefly introduce the quasiclassical theory. We then describe in detail the boundary conditions used in this work, and discuss our choice of the scattering matrix and its properties. In section III we first present our results for mirror junction: We study the temperature dependent critical current for interfaces with varying roughness and make a quantitative comparison with experimental data. We furthermore examine the transition to a  $\pi$ -junction, where a spontaneous current parallel to the

junction is present. Secondly we present the results for 45° asymmetric junctions, where additionally to the average quantities also statistical fluctuation of the critical current are examined. In both cases we discuss in detail the influence of interface roughness, which might lead to clear modifications of the results for the clean case. Concluding remarks are given in section IV.

## II. METHOD

In this section we introduce the main ingredients for our phenomenological model of rough superconducting contacts: The superconducting state is described by the quasiclassical theory, which is supplemented by boundary conditions to take into account interface scattering. We first recall the basic formalism.

### A. Theory of quasiclassical Green's functions

The quasiclassical matrix Green's function is determined by the Eilenberger equation which in thermal equilibrium reads

$$\left[ \hat{\tau}_3 E + e \hat{\tau}_3 \mathbf{v}_F \cdot \mathbf{A}(\mathbf{r}) + i \hat{\Delta}(\mathbf{p}_F, \mathbf{r}), \hat{g}(E, \mathbf{p}_F; \mathbf{r}) \right] + i \mathbf{v}_F \cdot \partial_{\mathbf{r}} \hat{g}(E, \mathbf{p}_F; \mathbf{r}) = 0. \quad (1)$$

Here  $\hat{\tau}_i$  are the Pauli matrices in Nambu space. The physically relevant solution is fixed by the normalization condition

$$[\hat{g}(E, \mathbf{p}_F; \mathbf{r})]^2 = \hat{1}. \quad (2)$$

The (spin-singlet) order parameter has the matrix form

$$\hat{\Delta}(\mathbf{p}_F, \mathbf{r}) = \begin{pmatrix} 0 & \Delta(\mathbf{p}_F, \mathbf{r}) \\ \Delta^*(\mathbf{p}_F, \mathbf{r}) & 0 \end{pmatrix} \quad (3)$$

and must be determined self-consistently via

$$\hat{\Delta}(\mathbf{p}_F, \mathbf{r}) = -\pi \mathcal{N}_0 T \sum_{|E_n| < E_c} \langle V(\mathbf{p}_F, \mathbf{p}'_F) \hat{g}(iE_n, \mathbf{p}'_F; \mathbf{r}) \rangle_{\mathbf{p}'_F}, \quad (4)$$

where  $E_n = \pi T(2n + 1)$  are the Matsubara energies ( $\hbar = k_B = 1$ ) and  $\mathcal{N}_0$  is the density of states (DOS) at the Fermi level in the normal state. For convenience we assume a cylindrical Fermi surface;  $\langle \dots \rangle_{\mathbf{p}_F}$  denotes the Fermi surface average. In the BCS approximation the pairing interaction is given by its strength  $V$ , its cut-off energy  $E_c$ , and its direction dependence which can be expanded for a  $d$ -wave order parameter as follows

$$V(\mathbf{p}_F, \mathbf{p}'_F) = V \eta(\mathbf{p}_F) \eta(\mathbf{p}'_F) \quad (5)$$

with

$$\eta(\mathbf{p}_F) = (p_{F,x}^2 - p_{F,y}^2) / p_F^2. \quad (6)$$

For a homogeneous system and temperature  $T = 0$  one finds  $\hat{\Delta}(\mathbf{p}_F, \mathbf{r}) = \hat{\tau}_1 \Delta_0 \eta(\mathbf{p}_F)$ , with  $\Delta_0 \approx 2.14 T_c$ .

Having solved these equations for the Green's function, various observables can be calculated. In this work the current density (in thermal equilibrium) is of particular interest:

$$\mathbf{j}(\mathbf{r}) = -ie\pi \mathcal{N}_0 T \sum_{n=-\infty}^{\infty} \text{Tr} \left[ \hat{\tau}_3 \langle \mathbf{v}_F \hat{g}(iE_n, \mathbf{p}_F; \mathbf{r}) \rangle_{\mathbf{p}_F} \right]. \quad (7)$$

Another important quantity is the DOS which is given by

$$\mathcal{N}(E, \mathbf{r}) = \langle \mathcal{N}(E, \mathbf{p}_F, \mathbf{r}) \rangle_{\mathbf{p}_F}, \quad (8)$$

with the angle-resolved DOS

$$\mathcal{N}(E, \mathbf{p}_F, \mathbf{r}) = \frac{1}{2} \mathcal{N}_0 \text{Re} \{ \text{Tr} [\hat{\tau}_3 \hat{g}(E + i0_+, \mathbf{p}_F; \mathbf{r})] \}. \quad (9)$$

In order to solve the Eilenberger equation it is useful to parameterize the Green's function as suggested in Refs.<sup>23,26,27</sup>

$$\hat{g} = \frac{1}{1 - ab} \begin{pmatrix} 1 + ab & -2a \\ 2b & -(1 + ab) \end{pmatrix}. \quad (10)$$

Note that the normalization condition is fulfilled by construction. The ansatz (10) yields the Riccati type equations for the amplitudes  $a(E, \mathbf{p}_F; \mathbf{r})$  and  $b(E, \mathbf{p}_F; \mathbf{r})$ :

$$\mathbf{v}_F \cdot \partial_{\mathbf{r}} a = \Delta^* a^2 + 2i(E + e \mathbf{v}_F \cdot \mathbf{A})a - \Delta, \quad (11)$$

$$\mathbf{v}_F \cdot \partial_{\mathbf{r}} b = \Delta b^2 - 2i(E + e \mathbf{v}_F \cdot \mathbf{A})b - \Delta^*. \quad (12)$$

The (numerical) evaluation of these amplitudes along classical trajectories  $\mathbf{r}(\lambda) = \mathbf{r}_0 + \lambda \mathbf{v}_F / v_F$  is more convenient than solving the Eilenberger Eq. (1) together with the normalization condition Eq. (2). In the case  $\text{Im}[E] > 0$ , i.e. for the retarded Green's function or the Matsubara Green's function with  $E_n > 0$ , the integration of Eq. (11) is stable in positive  $\mathbf{v}_F$ -direction, and Eq. (12) is stable in negative  $\mathbf{v}_F$ -direction; the directions must be reversed for  $\text{Im}[E] < 0$ . In the cases considered here the trajectories start and end in the bulk ( $\lambda = \pm\infty$ ) where the order parameter has no spatial dependence; then Eqs. (11) and (12) yield the homogeneous solutions ( $\partial_{\mathbf{r}} a = 0, \partial_{\mathbf{r}} b = 0$ )

$$a(E, \mathbf{p}_F; \lambda \rightarrow -\infty) = \frac{-i\Delta_-(\mathbf{p}_F)}{E + \sqrt{E^2 - |\Delta_-(\mathbf{p}_F)|^2}}, \quad (13)$$

$$b(E, \mathbf{p}_F; \lambda \rightarrow +\infty) = \frac{i\Delta_+(\mathbf{p}_F)}{E + \sqrt{E^2 - |\Delta_+(\mathbf{p}_F)|^2}}, \quad (14)$$

where  $\Delta_{\pm}(\mathbf{p}_F)$  is the order parameter for  $\lambda \rightarrow \pm\infty$ . Starting from these initial values Eqs. (11) and (12) must be integrated in positive and negative directions, respectively. It is then possible to construct the Green's function on the trajectory via Eq. (10).

In the following subsection we show that this parameterization is a good starting point for implementing boundary conditions which are necessary to study interfaces.

## B. Boundary conditions

The amplitudes  $a$  with  $\mathbf{p}_F$  pointing towards the interface (in-direction) can be calculated by integrating Eq. (11) with the initial value in the bulk given by Eq. (13); analogously the  $b$ 's with  $\mathbf{p}_F$  pointing away from the interface (out-direction) can be calculated via Eqs. (12) and (14). The boundary conditions provide the  $a$ 's in out-direction and the  $b$ 's in in-direction directly at the interface; starting with these values the integration of Eqs. (11) and (12), respectively, yields the  $a$ 's in the out- and the  $b$ 's in the in-direction.

For simplicity we consider only a finite number  $n$  of trajectories on each side of the junction, i.e.  $\mathbf{p}_{F\text{in/out}}^s \rightarrow \mathbf{p}_{F\text{in/out}}^{s,i}$  ( $i = 1, \dots, n$ ,  $s = l/r$ : left/right); we choose the numbering of the directions such that (see Fig. 1)

$$\mathbf{p}_{F\text{in},y}^{l,i} = \mathbf{p}_{F\text{out},y}^{l,i} = \mathbf{p}_{F\text{in},y}^{r,i} = \mathbf{p}_{F\text{out},y}^{r,i}. \quad (15)$$

We denote the amplitude  $a$  on the  $i^{\text{th}}$  in/out-trajectory on the side  $s$  of the junction by  $a_{\text{in/out}}^{s,i}$ , and  $b_{\text{in/out}}^{s,i}$  analogously. To formulate the boundary conditions we follow Ref.<sup>28</sup> by introducing the determinant  $\mathcal{D}$  as follows:

$$\mathcal{D}(\{a_{\text{in}}^{s,i}\}, \{b_{\text{out}}^{s,i}\}) = \det(\mathbf{1} - \mathbf{S}\mathbf{a}\mathbf{S}^\dagger\mathbf{b}) ; \quad (16)$$

the  $2n \times 2n$  diagonal matrices  $\mathbf{a}$  and  $\mathbf{b}$  read

$$\mathbf{a} = \text{diag}[\{a_{\text{in}}^{l,i}\}, \{a_{\text{in}}^{r,i}\}], \quad (17)$$

$$\mathbf{b} = \text{diag}[\{b_{\text{out}}^{l,i}\}, \{b_{\text{out}}^{r,i}\}], \quad (18)$$

where the  $a$ 's and  $b$ 's are the amplitudes at the interface ( $x = 0$ ). The unitary  $2n \times 2n$  scattering matrix  $\mathbf{S}$ , which contains the physical properties of the interface, has the block structure

$$\mathbf{S} = \begin{pmatrix} \mathbf{S}^{ll} & \mathbf{S}^{lr} \\ \mathbf{S}^{rl} & \mathbf{S}^{rr} \end{pmatrix}, \quad (19)$$

where the elements are  $n \times n$  matrices. As described in detail in<sup>28</sup> we define the quantities

$$\mathcal{A}_0^{s,i} = \mathcal{D} \Big|_{a_{\text{in}}^{s,i}=0}, \quad \mathcal{A}_1^{s,i} = \frac{\partial \mathcal{D}}{\partial a_{\text{in}}^{s,i}} \Big|_{a_{\text{in}}^{s,i}=0}, \quad (20)$$

$$\mathcal{B}_0^{s,i} = \mathcal{D} \Big|_{b_{\text{out}}^{s,i}=0}, \quad \mathcal{B}_1^{s,i} = \frac{\partial \mathcal{D}}{\partial b_{\text{out}}^{s,i}} \Big|_{b_{\text{out}}^{s,i}=0}. \quad (21)$$

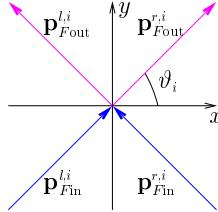


FIG. 1: At an specular interface the Green's functions on the four trajectories with the same parallel momentum  $p_{F,y}$  are coupled coherently.

The boundary conditions yield the unknown values of  $a$  and  $b$  at the interface via

$$a_{\text{out}}^{s,i} = -\frac{\mathcal{B}_1^{s,i}}{\mathcal{B}_0^{s,i}}, \quad b_{\text{in}}^{s,i} = -\frac{\mathcal{A}_1^{s,i}}{\mathcal{A}_0^{s,i}}. \quad (22)$$

To apply these boundary conditions to interfaces, we must ensure current conservation across the junction. As discussed in Ref.<sup>28</sup> the above boundary conditions yield the following conservation law:

$$\begin{aligned} & \sum_{i=1}^n [\tilde{j}^l(E, \mathbf{p}_{F\text{in}}^{l,i}) - \tilde{j}^l(E, \mathbf{p}_{F\text{out}}^{l,i})] \\ &= \sum_{i=1}^n [\tilde{j}^r(E, \mathbf{p}_{F\text{out}}^{r,i}) - \tilde{j}^r(E, \mathbf{p}_{F\text{in}}^{r,i})] \end{aligned} \quad (23)$$

where the contribution of each direction is given by

$$\tilde{j}^s(E, \mathbf{p}_F) = \text{Tr}[\hat{\tau}_3 \hat{g}^s(E, \mathbf{p}_F; 0)]. \quad (24)$$

On the other hand, we impose current conservation perpendicular to the junction (see Eq. (7))

$$\begin{aligned} & \langle v_{F,x} [\tilde{j}^l(E, \mathbf{p}_{F\text{in}}^l) - \tilde{j}^l(E, \mathbf{p}_{F\text{out}}^l)] \rangle_{\mathbf{p}_{F\text{in}}^l} \\ &= \langle v_{F,x} [\tilde{j}^r(E, \mathbf{p}_{F\text{in}}^r) - \tilde{j}^r(E, \mathbf{p}_{F\text{out}}^r)] \rangle_{\mathbf{p}_{F\text{in}}^r}. \end{aligned} \quad (25)$$

Note that the directions  $\mathbf{p}_{F\text{in}}^{s,i}$  and  $\mathbf{p}_{F\text{out}}^{s,i}$  are related by Eq. (15), see Fig. 1. To ensure current conservation perpendicular to the junction, we construct the grid of the discrete directions so that the term  $v_{F,x} = v_F p_{F,x}/p_F$  is already taken into account. This is guaranteed by choosing the grid as

$$\begin{aligned} \mathbf{p}_{F\text{in}}^{l,i} &= p_F \begin{pmatrix} \cos \vartheta_i \\ \sin \vartheta_i \end{pmatrix}, & \mathbf{p}_{F\text{in}}^{r,i} &= p_F \begin{pmatrix} -\cos \vartheta_i \\ \sin \vartheta_i \end{pmatrix}, \\ \mathbf{p}_{F\text{out}}^{l,i} &= p_F \begin{pmatrix} -\cos \vartheta_i \\ \sin \vartheta_i \end{pmatrix}, & \mathbf{p}_{F\text{out}}^{r,i} &= p_F \begin{pmatrix} \cos \vartheta_i \\ \sin \vartheta_i \end{pmatrix}, \\ \sin \vartheta_i &= \frac{2i}{n+1} - 1, & i &= 1, \dots, n. \end{aligned} \quad (26)$$

In other words this grid takes into account that the rate of scattering events at the interface decreases with smaller angles of incidence.

The probability of scattering from the direction  $\mathbf{p}_{F\text{in}}^{s,j}$  into an interval  $[\mathbf{p}_{F\text{out}}^{s',i}, \mathbf{p}_{F\text{out}}^{s',i+1}]$  ( $s, s' = l/r$ ) reads

$$P_{s's}(\vartheta_j \rightarrow \vartheta_i) \Delta \vartheta_i = |S_{ij}^{s's}|^2, \quad (27)$$

with  $\Delta \vartheta_i = \vartheta_i - \vartheta_{i-1}$ . Using the non-equidistant grid as defined in Eq. (26) for a large number of scattering channels,  $n \gg 1$ , we find

$$P_{s's}(\vartheta_j \rightarrow \vartheta_i) = \frac{n}{2} \cos \vartheta_i |S_{ij}^{s's}|^2. \quad (28)$$

In the next step one has to find the appropriate scattering matrices for a given physical realization. In the following subsection we study the case of a specular and an irregular rough interface.

### C. Scattering matrix

The most simple case is a specular interface where only trajectories with the same parallel momentum are coupled. Then the block matrices that form the scattering matrix in Eq. (19) have diagonal form:

$$\begin{aligned} \mathbf{S}^{ll} &= -\mathbf{S}^{rr} = \mathbf{R} = \text{diag} \left[ \sqrt{1 - \mathcal{T}(\vartheta_i)} \right], \\ \mathbf{S}^{lr} &= \mathbf{S}^{rl} = \mathbf{T} = \text{diag} \left[ \sqrt{\mathcal{T}(\vartheta_i)} \right]; \end{aligned} \quad (29)$$

in particular, for a  $\delta$ -like boundary potential the direction-dependent transparency reads<sup>29</sup>

$$\mathcal{T}(\vartheta) = \frac{\mathcal{T}_0 \cos^2 \vartheta}{1 - \mathcal{T}_0 \sin^2 \vartheta}, \quad \mathcal{T}_0 \in [0, 1]. \quad (30)$$

For a normal metal this leads to the resistance of the tunnel-barrier

$$R_N^{-1} = \frac{4Ae^2 \mathcal{N}_0 v_F}{3\pi} \mathcal{T}_0, \quad (31)$$

where  $A$  is the area of the contact<sup>25</sup>.

In the superconducting case the boundary conditions for a specular interface can be solved for each direction individually, with the result<sup>23,30</sup>

$$a_{\text{out}}^{s,i} = \frac{a_{\text{in}}^{\bar{s},i} \mathcal{T}_i (1 - a_{\text{in}}^{s,i} b_{\text{out}}^{\bar{s},i}) + a_{\text{in}}^{s,i} \mathcal{R}_i (1 - a_{\text{in}}^{\bar{s},i} b_{\text{out}}^{\bar{s},i})}{\mathcal{T}_i (1 - a_{\text{in}}^{s,i} b_{\text{out}}^{\bar{s},i}) + \mathcal{R}_i (1 - a_{\text{in}}^{\bar{s},i} b_{\text{out}}^{\bar{s},i})}, \quad (32)$$

$$b_{\text{in}}^{s,i} = \frac{b_{\text{out}}^{\bar{s},i} \mathcal{T}_i (1 - a_{\text{in}}^{\bar{s},i} b_{\text{out}}^{s,i}) + b_{\text{out}}^{s,i} \mathcal{R}_i (1 - a_{\text{in}}^{\bar{s},i} b_{\text{out}}^{s,i})}{\mathcal{T}_i (1 - a_{\text{in}}^{\bar{s},i} b_{\text{out}}^{s,i}) + \mathcal{R}_i (1 - a_{\text{in}}^{\bar{s},i} b_{\text{out}}^{s,i})} \quad (33)$$

where  $s = l/r$ ,  $\bar{s} = r/l$ , respectively, and  $\mathcal{T}_i = \mathcal{T}(\vartheta_i)$ ,  $\mathcal{R}_i = 1 - \mathcal{T}_i$ .

A rough surface, on the other hand, is described by a scattering matrix that does not only depend on the transparency but also on a roughness parameter. Our starting point to construct such a unitary scattering matrix is<sup>31</sup>

$$\mathbf{S} = \begin{pmatrix} \mathbf{U}_1 & 0 \\ 0 & \mathbf{U}_2 \end{pmatrix} \begin{pmatrix} \mathbf{T} & \mathbf{R} \\ \mathbf{R} & -\mathbf{T} \end{pmatrix} \begin{pmatrix} \mathbf{U}_3 & 0 \\ 0 & \mathbf{U}_4 \end{pmatrix}, \quad (34)$$

with  $\mathbf{R}$  and  $\mathbf{T}$  as defined in Eq. (29), which contain the information on the transparency. The unitary matrices  $\mathbf{U}_k$  describe the interface roughness; for  $\mathbf{U}_k = \mathbf{1}$  the scattering matrix for a specular interface obviously is recovered.

We will focus on interfaces without regular structure. To take into account the statistical character of rough interfaces we choose the  $\mathbf{U}_k$  to be unitary random matrices<sup>24,25</sup>,

$$\mathbf{U}_k = \exp\{i\mathbf{H}_k\}, \quad (35)$$

where each  $\mathbf{H}_k$  is a random matrix with Gaussian correlations:

$$\langle H_{k,ij} \rangle = 0, \quad \langle H_{k,ij}^* H_{k',i'j'} \rangle = \frac{\tau}{2n} \delta_{ii'} \delta_{jj'} \delta_{kk'}. \quad (36)$$

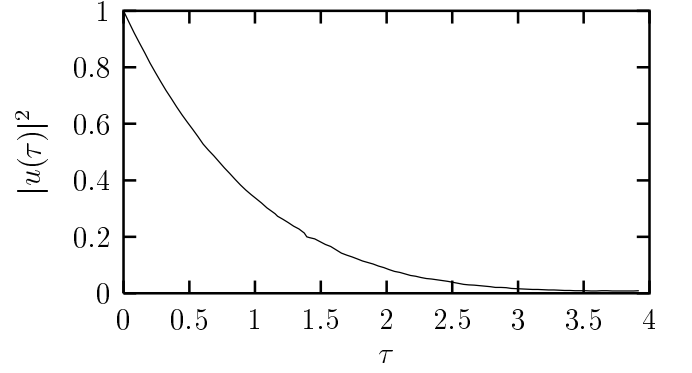


FIG. 2: The weight for specular scattering,  $|u|^2$ , decreases with growing  $\tau$ ; for  $\tau \gtrsim 3$  specular scattering is almost completely suppressed ( $|u|^2 \ll 1$ ).

Here  $\langle \dots \rangle$  denotes the disorder average. In the following we use the abbreviations

$$|u(\tau)| = \langle |U_{k,ii}|^2 \rangle, \quad |v(\tau)| = \langle |U_{k,i \neq j}|^2 \rangle \quad (37)$$

to describe the average scattering probability; due to the unitarity it follows that  $|u| + (n-1)|v| = 1$ . Obviously for  $\tau = 0$  we find  $|u(\tau)| = 1$ , whereas for increasing (positive)  $\tau$ , we obtain a reduced value,  $|u(\tau)| < 1$ , as can be seen in Fig. 2. A detailed discussion can be found in<sup>25</sup>.

Using Eq. (28) we find the average transmission probability density for scattering from the direction  $\mathbf{p}_{F\text{in}}^{s,j}$  on one side of the junction to  $\mathbf{p}_{F\text{out}}^{\bar{s},i}$  on the other side,

$$\begin{aligned} \langle P_{s\bar{s}}(\vartheta_j \rightarrow \vartheta_i) \rangle &= \frac{\cos \vartheta_i}{2} \left\{ n |u|^2 \mathcal{T}(\vartheta_i) \delta_{ij} + \kappa (1 - |u|)^2 \right. \\ &\quad \left. + |u| (1 - |u|) [\mathcal{T}(\vartheta_i) + \mathcal{T}(\vartheta_j)] (1 - \delta_{ij}) \right\}, \end{aligned} \quad (38)$$

with

$$\kappa = \frac{1}{n} \sum_i \mathcal{T}(\vartheta_i) \rightarrow \begin{cases} \mathcal{T}_0/2 & \text{for } \mathcal{T}_0 \ll 1 \\ 1 & \text{for } \mathcal{T}_0 = 1 \end{cases}. \quad (39)$$

Furthermore the reflection probabilities  $\langle P_{ss} \rangle$  can easily be obtained by substituting  $\mathcal{T} \rightarrow (1 - \mathcal{T})$  and  $\kappa \rightarrow (1 - \kappa)$  in Eq. (38). The continuum limit of Eq. (38) reads

$$\begin{aligned} \langle P_{s\bar{s}}(\vartheta \rightarrow \vartheta') \rangle &= |u|^2 \mathcal{T}(\vartheta') \delta(\vartheta' - \vartheta) + \\ &\quad + \frac{\cos \vartheta'}{2} \left\{ \kappa (1 - |u|)^2 + |u| (1 - |u|) [\mathcal{T}(\vartheta') + \mathcal{T}(\vartheta)] \right\}; \end{aligned} \quad (40)$$

note that the weight of specular scattering is determined by the quantity  $|u|^2$ : For a specular interface ( $\tau = 0$ ) it is  $|u|^2 = 1$ , whereas in the very rough limit ( $\tau \gg 1$ ) we find  $|u|^2 \rightarrow 0$  (see Fig. 2).

So far we discussed the boundary conditions at a single point of an interface for a discrete number of directions  $\mathbf{p}_F$ . A real interface will have a finite cross section and

the directions will be continuous. Therefore the question arises how these boundary conditions can be applied to real interfaces.

First we consider the discretization of the Fermi surface. A finite number  $n$  sets the typical angle,  $\vartheta_c \approx \pi/n$ , over which the scattering probability can vary. For small  $\vartheta_c$  the fluctuations of the scattering probability with varying directions are averaged out more effectively by the Fermi surface average that must be taken to evaluate observables such as the current or the order parameter. Therefore the self-averaging character of the physical quantities increases with decreasing  $\vartheta_c$ ; i.e. the statistical fluctuations of physical quantities are diminished for a small  $\vartheta_c$ . It is important to note that only the statistical fluctuations of physical quantities depend on the value of  $\vartheta_c$ , but that the mean values are independent of  $\vartheta_c$ , as long as  $\vartheta_c \ll \pi$ . Throughout the following calculations we choose  $n = 40$ .

Second we comment on the number of different realizations of the scattering matrix that must be taken into account. In the original formulation of boundary conditions by Shelankov and Ozana<sup>23</sup> the spatial resolution is limited by the Fermi wave length,  $1/p_F$ ; therefore the number of different realizations should be of the order  $Ap_F^2$ , where  $A$  is the area of the contact. On the other hand, we expect that quantities like the current density or the order parameter, which are of interest to us, vary on the scale of the coherence length,  $\xi_0$ . Therefore we choose one effective scattering matrix  $\mathbf{S}$  to describe an area  $\xi_0^2$  of the whole contact. As the order parameter relaxes on the coherence length it is reasonable to treat each of these areas individually neglecting the influence from other part of the contact; this approximation considerably simplifies the self-consistent treatment of the quasiclassical theory. Finally the current perpendicular to a junction of area  $A$  is calculated via

$$I_x = \int_A dA j_x(\mathbf{r}) \approx \xi_0^2 \sum_{i=1}^{A/\xi_0^2} j_{x,i}, \quad (41)$$

where each  $j_{x,i}$  is evaluated for one particular realization of the scattering matrix. For large junctions ( $A \gg \xi_0^2$ ) the current is given by the average over many scattering matrices; for smaller junctions ( $A$  of the order of  $\xi_0^2$  or even smaller) statistical fluctuations become relevant.

### III. RESULTS AND DISCUSSION

We consider two kinds of Josephson junctions. First we discuss so-called mirror junctions where the order parameter on both sides is rotated by the same angle  $\alpha$  but in opposite directions (see Fig. 3). Second we examine the  $45^\circ$  asymmetric junction where the order parameter is rotated only on the right hand side (see Fig. 4).

We recall the general expansion of the current-phase relation between two superconductors,

$$I_x(T, \varphi) = I_1(T) \sin \varphi + I_2(T) \sin(2\varphi) + \dots \quad (42)$$

with the superconducting phase difference,  $\varphi$ , between the left and the right hand side. It is also worth mentioning that the current-phase can be obtained from the free energy of the junction via

$$I_x(T, \varphi) = 2|e| \frac{\partial}{\partial \varphi} \mathcal{F}(T, \varphi). \quad (43)$$

Besides their temperature dependence, the contributions  $I_k$  scale as

$$I_k \propto \mathcal{T}_0^k \quad (44)$$

for small transparencies. For  $s$ -wave superconductors and small enough  $\mathcal{T}_0$  only the linear term in the transparency,  $I_1$ , is relevant. In the following we will show that this needs not be the case for  $d$ -wave superconductors.

#### A. Mirror junction

In this section we will consider mirror junctions, which are schematically illustrated in Fig. 3. For a junction with purely specular scattering, a particular symmetry is present, which reads

$$\begin{aligned} \Delta^l(\mathbf{p}_{Fin}^l) &= \Delta^r(\mathbf{p}_{Fin}^r), \\ \Delta^l(\mathbf{p}_{Fout}^l) &= \Delta^r(\mathbf{p}_{Fout}^r). \end{aligned} \quad (45)$$

This means that for a given incoming trajectory the order parameter is identical for the transmitted and the reflected quasi-particle. All directions can therefore be divided into two classes: (i) For some directions the sign of the order parameter is the same for all involved trajectories ( $\Delta^l(\mathbf{p}_{Fin}^l)\Delta^l(\mathbf{p}_{Fout}^l) > 1$ ). The behavior of these directions is similar to that of usual  $s$ -wave superconductors: Their contribution to  $I_1$  is positive and finite for  $T < T_c$ . (ii) For the other directions the sign for the in- compared to the out-trajectories changes ( $\Delta^l(\mathbf{p}_{Fin}^l)\Delta^l(\mathbf{p}_{Fout}^l) < 0$ ). This has two crucial consequences: These directions have a negative contribution to  $I_1$  which moreover diverges in the tunnel limit as  $1/T$  for  $T \rightarrow 0$ . The reason for this divergence is the existence

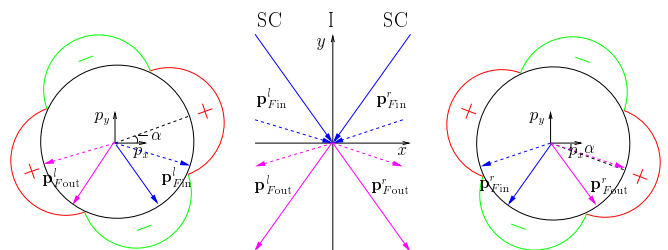


FIG. 3: For mirror junctions the order parameter on the left and the right hand side of the junction are rotated by the same angle  $\alpha$  but in opposite directions. For specular scattering the order parameters on both in-trajectories and out-trajectories, respectively, are equal.

of Andreev bound states near zero energy at the interface as the reflected quasi-particles acquire a sign change of the order parameter<sup>5,25</sup>; the divergence is cut-off by a finite transparency, which leads to a shift of the bound state to finite energies, and by disorder, which leads to a broadening of the level.

Altogether the  $s$ -wave-like contributions dominate for high temperatures, which, for a fixed phase difference  $0 < \varphi < \pi$ , leads to a positive current, whereas for low temperature the anomalous contributions are enhanced, which results in a negative current. In other words, the ground state of the junction shifts from  $\varphi = 0$  (0-junction) to  $\varphi = \pi$  ( $\pi$ -junction) when decreasing the temperature. This transition occurs at the temperature  $T_\pi$ , where both contributions cancel; at this temperature, the leading  $\sin \varphi$ -like contribution vanishes ( $I_1 = 0$ ) and the junction is dominated by higher order terms. As the amount of directions preferring a  $\pi$ -junction increases with a growing angle  $\alpha$ , also the temperature  $T_\pi$  increases with  $\alpha$ .

In the following we will discuss the influence of interface roughness on the temperature dependence of the critical current. We calculate the current contributions  $I_1$  and  $I_2$  as defined in Eq. (42); higher order contributions,  $I_k$ ,  $k > 2$ , can be neglected as we consider only small transparencies. We determine the critical current,  $I_c$ , from the absolute maximum of the current phase relation. In the graphs a  $\pi$ -junction behavior is indicated by a negative value. It should be mentioned that in experiments the absolute value,  $|I_c|$  is measured, thus a minimum in the temperature dependent critical current is observed at  $T = T_\pi$ . We focus on the case  $\alpha = 22.5^\circ$ ; for the presented results the transparency is set to  $\mathcal{T}_0 = 0.01$ . The average current is evaluated by using 20 realizations of the scattering matrix; the statistical error is less than 10%.

First, we concentrate on the clean case. There, as mentioned above, the directions preferring a  $\pi$ -junction and those preferring a 0-junction compete: From the temperature dependence of the critical current, as shown in Fig. 5, we find a  $\pi$ -junction behavior below  $T_\pi \approx 0.36 T_c$ , whereas for high temperatures the 0-junction state is favored. Recalling Eq. (43), the shift of the ground state from  $\varphi = 0$  to  $\varphi = \pi$  can be seen in the current-phase relation for decreasing temperature near  $T_\pi$  (see Fig. 6).

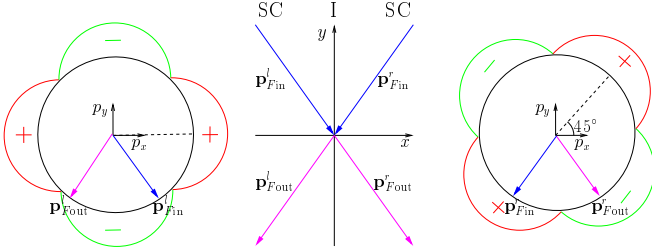


FIG. 4: For a  $45^\circ$  asymmetric junction the order parameter is tilted on one side only.

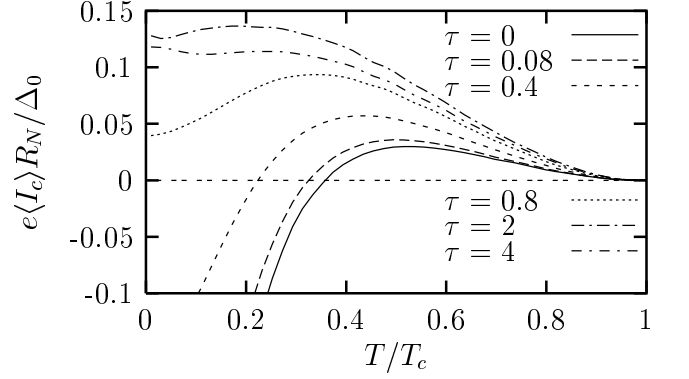


FIG. 5: Critical current for a mirror junction with  $\mathcal{T}_0 = 0.01$  and  $\alpha = 22.5^\circ$ . Negative values indicate a  $\pi$ -junction state. Near  $T = T_\pi$  the plotted curves make a jump from a positive to a negative value and hence the critical current stays finite. Due to the small transparency the jump is not visible in this plot but in Fig. 6.

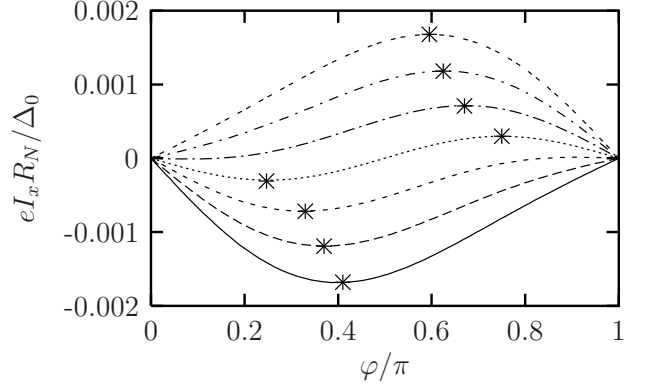


FIG. 6: Current phase relation of a mirror junction without roughness ( $\mathcal{T}_0 = 0.01$ ,  $\alpha = 22.5^\circ$ ) near the temperature where it becomes a  $\pi$ -junction ( $T = T_\pi \pm k \cdot 10^{-3} T_c$ ,  $k = 0, 1, 2, 3$ , increasing  $T$  from bottom to top). The asterisks mark the points which define the critical current. Note that the critical current remains finite at  $T = T_\pi$  due to the  $\sin(2\varphi)$ -like contribution.

In particular a finite critical current can be observed even for  $T = T_\pi$ , since the contribution  $I_2$  remains finite, whereas  $I_1$  vanishes. In Fig. 5 the jump in the current at  $T = T_\pi$  is too small to be visible; the reason is the tiny transparency ( $\mathcal{T}_0 = 0.01$ ) we used in this calculation. Moreover it can be seen in Fig. 6 that the current-phase relation at  $T_\pi$  is  $\sin(2\varphi)$ -like, which is related to the degeneracy of the ground state. The ground state exhibits a non-trivial phase difference  $\varphi = \pi/2, 3\pi/2$  which leads to a current parallel to the interface; notice that also the anisotropy of the order parameter plays a crucial role such that the contributions with opposite  $y$ -component do not cancel each other. The parallel current is presented in Fig. 7, where we use  $j_0 = 2e\mathcal{N}_0 v_F \Delta_0$  as a unit for the current density. We should mention that the current scales with the transparency of the contact,  $\mathcal{T}_0$ . For other orientations of the order parameter,  $\alpha < 22.5^\circ$ , the



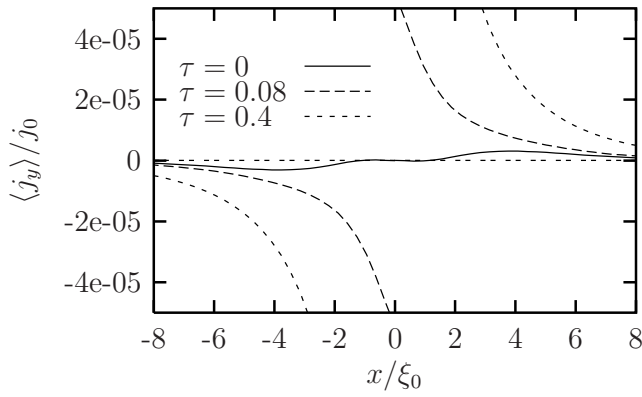


FIG. 7: Ground state current in  $y$ -direction at a mirror junction with  $\alpha = 22.5^\circ$  and  $T_0 = 0.01$  at  $T = T_\pi$ , i.e.  $\varphi \approx \pi/2$ . The current density is increasing with the roughness of the interface.

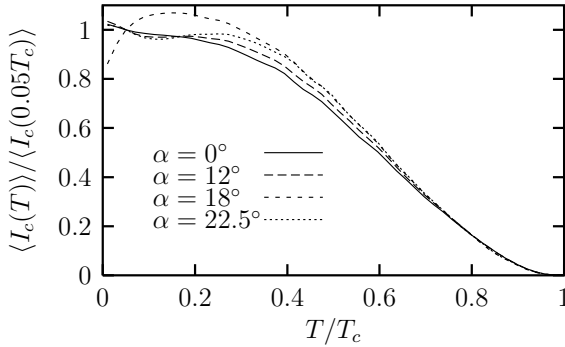


FIG. 8: Critical current of mirror junction with different orientation for very rough interfaces ( $\tau = 4$ ). The temperature dependence of  $I_c(T)/I_c(0.05T_c)$  is monotonic (within the numerical error) and its angle dependence is only weak.

same qualitative behavior should be observed but with a reduced  $T_\pi$ .

Obviously, roughness suppresses the  $\pi$ -junction behavior (see Fig. 5). With increasing  $\tau$ , the temperature  $T_\pi$  decreases until the transition disappears for very rough interfaces. This can be understood as follows: The negative current contributions are carried by Andreev bound states with  $E \lesssim 0$ <sup>5</sup>; as they are broadened by disorder<sup>25</sup> their negative current contribution is partially canceled by those bound states with  $E \gtrsim 0$ . Due to this suppression of the  $\pi$ -junction contribution at rough interfaces, the normal 0-junction contribution becomes dominant also for lower temperatures; this contribution is more stable against roughness as it is carried by bound states at  $E \gtrsim -|\Delta|^5$ . For large enough disorder we finally find  $I_1 > 0$  in the whole temperature range. When further increasing the roughness the critical current is enhanced until the negative contributions vanish completely. Then, the temperature dependence of the critical current, i.e.  $I_c(T)/I_c(0.05T_c)$ , has a monotonic shape almost as in the  $s$ -wave case. For a very rough interface the quantity

$I_c(T)/I_c(0.05T_c)$  depends only weakly on the orientation,  $\alpha$  (see Fig. 8).

Also with disorder the ground state at  $T = T_\pi$  (as long as  $T_\pi > 0$ ) exhibits a finite phase difference, which leads to a spontaneous current parallel to the interface. As shown in Fig. 7 the current density increases rapidly with growing interface roughness. This can be understood as follows: In the clean case the directions preferring a 0-junction and those preferring a  $\pi$ -junction contribute to the current with opposite sign; this leads to a partial cancellation also of the parallel current. As discussed before, roughness suppresses the  $\pi$ -junction behavior; as a consequence the cancellation of the current contributions is less effective, hence the current increases with roughness. It should be mentioned that for this type of junction ( $\alpha = 22.5^\circ$ ) the modification of the order parameter is small and plays only a minor role.

The suppression of the  $\pi$ -junction behavior by disorder has been reported earlier for alternative models of interface roughness<sup>6,19</sup>.

In the following, we will compare our results for the critical current with the experimental data of Refs.<sup>8,9,14,32</sup>. There a monotonic temperature dependence of the ratio  $I(T)/I(0.05T_c)$  has been reported, in agreement with our observations for very rough interfaces. The quantitative agreement of these results with the data reported in<sup>9</sup> for YBCO-junctions is reasonable for small angles,  $\alpha$ , whereas for larger angles it is quite poor; this can be seen when comparing the values of  $R_N I_c$  at  $T = 4.2$  K  $\approx 0.05 T_c$  (see table I). The discrepancy between our results and the experimental data might be related to facets on  $\mu\text{m}$ -scale at the interface<sup>15,34</sup>, which have an increasing influence for larger angles  $\alpha$ , as more facets yield a negative current contribution<sup>34</sup>. An average over all facet orientations then leads to a diminished total current.

Recently, for a small junction (width  $0.5\mu\text{m}$ ) with  $\alpha = 22.5^\circ$  a non-monotonic temperature dependence of the critical current has been reported<sup>13</sup> which, as already discussed, appears due to the transition to a  $\pi$ -junction for low temperatures. The minimum of the critical current was found for  $T_\pi = 12$  K  $= 0.13 T_c$ . The transparency is quite high, as can be seen from the large  $I_2$ -contribution. The measurement is in qualitative agree-

$\alpha$	$AR_N(\Omega\text{cm}^2)$ Ref. <sup>9</sup>	$\mathcal{T}_0^{\text{exp}}$	$R_N I_c(\text{mV})$ Ref. <sup>9</sup>	$R_N I_c(\text{mV})$ calculated
$12^\circ$	$5.4 \times 10^{-9}$	0.024	1.3	3.6
$18^\circ$	$1.5 \times 10^{-8}$	0.008	0.75	2.6
$22.5^\circ$	$1.2 \times 10^{-8}$	0.011	0.13	1.9

TABLE I: Comparison of experimental results for  $R_N I_c$  with calculated values. The transparency in the experiment,  $\mathcal{T}_0^{\text{exp}}$ , is estimated via Eq. (31) leading to the values  $AR_N$  given in the table, and  $v_F = 4.34 \times 10^6 \text{cm/s}$ ,  $\mathcal{N}_0 = 2.13 \times 10^{22}/\text{cm}^3 \text{eV}^{33}$ . For the calculations we used  $T_0 = 0.01$  (tunnel-limit),  $T = 0.05 T_c$ , and  $\tau = 4$ .

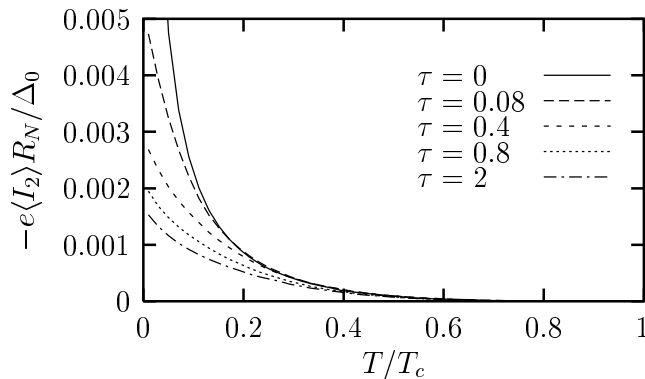


FIG. 9: Average current  $I_2$  for an asymmetric junction with  $\mathcal{T}_0 = 0.01$  and varying strength of the roughness; interface roughness suppresses the current  $I_2$ .

ment with results obtained from our model for  $\mathcal{T}_0 \gtrsim 0.2$  and  $\tau \gtrsim 0.4$ . It is also worth mentioning that this transition was observed for some of the samples only, which might be due to the sensitivity of mesoscopic junctions to fluctuations of the interface properties. Note that here facets are of minor importance, as the width of the junction is comparable to the typical facet size; so it is possible to have junctions with well-defined orientation.

In summary, we showed that the behavior of mirror junctions can be modified drastically by interface roughness: If the roughness is weak and the angle  $\alpha$  is large enough, a transition to a  $\pi$ -junction at low temperatures can be observed; near the transition temperature,  $T_\pi$ , the junction has a  $\sin(2\varphi)$ -like current-phase relation. For larger roughness the  $\pi$ -junction behavior is destroyed and the quantity  $I_c(T)/I_c(0.05T_c)$  depends only weakly on the orientation  $\alpha$ . When comparing with experimental data, we find qualitative agreement with our theory. However, especially the influence of large facets has to be taken into account to determine the absolute value of the critical current correctly.

### B. 45° asymmetric junction

For a clean 45° asymmetric junction, the particular geometric symmetry is responsible for a vanishing leading current contribution  $I_1$ : The symmetry operation  $y \rightarrow -y$  leads to a phase-shift  $\varphi \rightarrow \varphi + \pi$ , while on the other hand, the current in  $x$ -direction must be invariant. We therefore find the following condition for the current:

$$I_x(\varphi) = I_x(\varphi + \pi) \quad \Leftrightarrow \quad I_{2k-1} = 0, \quad k \in \mathbb{N}, \quad (46)$$

and the current-phase relation takes the form

$$I_x(\varphi) = I_2 \sin(2\varphi) + I_4 \sin(4\varphi) + \dots \quad (47)$$

This means that in the absence of disorder the current is dominated by the contribution  $I_2 \sin(2\varphi)$ . Asymmetric junctions therefore have two degenerate ground states

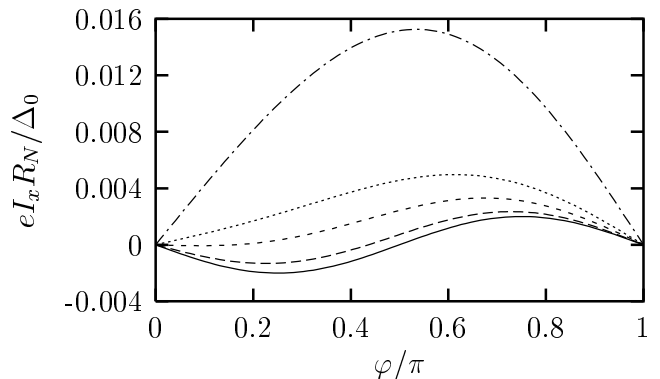


FIG. 10: Current-phase relation for single realizations of the disorder for an asymmetric junction with  $T = 0.1T_c$ . The transparency is  $\mathcal{T}_0 = 0.01$  and the roughness is given by the same parameters  $\tau$  as in Fig. 9.

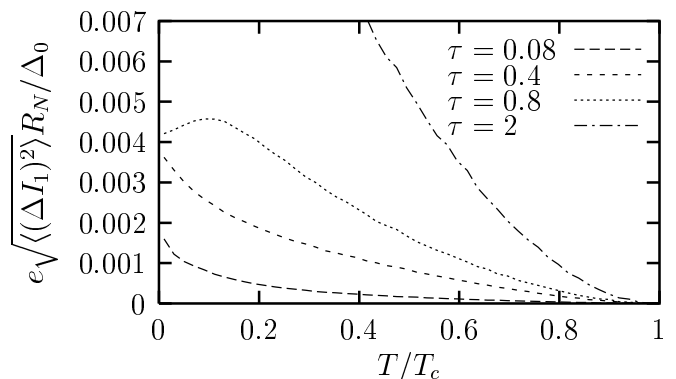


FIG. 11: Standard deviation of the current  $I_1$  for an asymmetric junction with  $\mathcal{T}_0 = 0.01$  and varying strength of the roughness,  $\vartheta_c \approx \pi/40$ ; this current contribution is increasing with the roughness.

at  $\varphi = \pi/2, 3\pi/2$ . For this reason such junctions are discussed as possible realizations of quantum bits<sup>35,36</sup>.

Considering rough interfaces we will first examine the average values of  $I_1$  and  $I_2$ ; later we will also discuss the statistical fluctuations and their relevance for physical realizations. We present data for a tunnel-junction ( $\mathcal{T}_0 = 0.01$ ). Moreover in our approach the statistical fluctuations depend on the angle  $\vartheta_c$  which is set to  $\vartheta_c \approx \pi/40$  (i.e.  $n = 40$  directions were taken into account).

Since, in our model for rough interfaces, the symmetry  $y \rightarrow -y$  is still present on average, it follows that  $\langle I_1 \rangle = 0$ ; i.e. on average the tunnel-current exhibits a  $\sin(2\varphi)$ -like current-phase relation.

The temperature dependence of  $\langle I_2 \rangle$  is shown in Fig. 9 for various roughness parameters. In the clean case for  $\mathcal{T}_0 \rightarrow 0$  and  $T \rightarrow 0$ , we find  $I_2 \propto 1/T$  due to the zero energy bound state at the interface; this state occurs as a result of the sign change of the order parameter for reflected quasi-particles on the right hand side. But finite roughness also leads to a suppression of this contribution and the average value  $\langle I_2 \rangle$  decreases with growing inter-



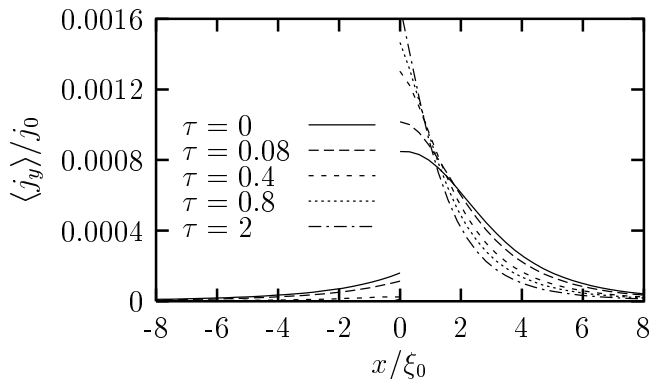


FIG. 12: Average ground state (i.e.  $\varphi \approx \pi/2$ ) current density in  $y$ -direction at an asymmetric junction with  $\mathcal{T}_0 = 0.01$ .

face roughness. As  $\langle I_1 \rangle = 0$  the ground state of the junction has a non-trivial phase difference  $\varphi = \pi/2, 3\pi/2$ , and hence the time-reversal symmetry is broken. Thus a current parallel to the interface exists (see Fig. 12) whereas no current in  $x$ -direction is present; as in the previous case the parallel current scales with transparency. The parallel current is carried by bound states at  $E \lesssim 0$ , which exist on both sides of the interface due to the finite transparency<sup>5</sup>; the bound states with  $E \gtrsim 0$  would contribute to the current in opposite direction, but they are not occupied. Interface roughness generally leads to a suppression of the parallel current since the bound states are broadened, and their current contributions tend to cancel each other. Only in a narrow region on the right hand side of the interface, of the order of the coherence length, the parallel current is enhanced, which is related to the considerable increase of the tilted order parameter at a rough interface<sup>25</sup>.

The average critical current of  $45^\circ$  asymmetric junctions was considered before for the clean<sup>3,37,38</sup> as well as for the rough case using the thin dirty layer model<sup>39</sup>. The results are similar to ours. The spontaneous parallel current was studied for the clean case<sup>38</sup>. Roughness was also considered for a completely transparent interface<sup>40</sup>, where a reduction of the parallel current was found for increasing roughness. The  $\sin(2\varphi)$ -like behavior has been observed in an experiment with a YBCO-junction by Il'ichev et al.<sup>12</sup>.

So far we assumed that the junction is well described by the average values of the current, but when considering a particular realization of the disorder (i.e. of the scattering matrix) the symmetry stated in Eq. (46) is no longer valid, and a finite contribution  $I_1$  is expected. To confirm this assertion we consider the current-phase relation for one particular scattering matrix at the temperature  $T = 0.1 T_c$ ; the result is shown in Fig. 10. The  $\sin(2\varphi)$ -behavior, observable in the clean case, is clearly modified by the roughness and a strong  $\sin \varphi$ -part additionally occurs; for  $\tau \gtrsim 0.4$  the current-phase relation is already dominated by this contribution. In order to study the statistical properties of the current more systemat-

ically we consider the standard deviation of the contribution  $I_1$ , namely  $\langle (\Delta I_1)^2 \rangle^{1/2}$ ; its temperature dependence is shown in Fig. 11. Even for small roughness the quantity  $\langle (\Delta I_1)^2 \rangle^{1/2}$  may already be of the same order of magnitude as  $\langle I_2 \rangle$ , in particular for higher temperatures (compare Figs. 9 and 11). The reason is the different dependence on the transparency of both contributions,  $I_1 \propto \mathcal{T}_0$  and  $I_2 \propto \mathcal{T}_0^2$ , so that for  $\mathcal{T}_0 \ll 1$  the contribution  $I_1$  dominates as soon as it is allowed by symmetry.

Recalling the physical meaning of the averaging process (see Sec. II C) we conclude that the statistical fluctuations should be relevant for small junctions ( $A$  of the order of  $\xi_0^2$  or even smaller), and a  $\sin \varphi$ -like current phase relation should be observable. On the other hand for large junctions ( $A \gg \xi_0^2$ ) the statistical fluctuations become irrelevant, and the behavior should be governed by the  $\sin(2\varphi)$ -like contribution. As already mentioned above a  $\sin(2\varphi)$ -like current-phase relation has been observed in experiment<sup>12</sup>. But only some of the samples showed this behavior; statistical fluctuations as discussed here can be ruled out as a reason, however, because the contact in the experiment is quite large compared to the coherence length of YBCO,  $\xi_0 \approx 15$  Å:  $A \approx 1 \mu\text{m} \times 100$  nm. A reasonable explanation might be a slight deviation from the  $45^\circ$ -orientation of the tilted order parameter in some samples, such that the contribution  $I_1$  is allowed by symmetry. Another explanation might be a faceted interface, so that for each facet the contribution  $I_1$  is finite.

#### IV. CONCLUSION

To describe a contact between two superconductors within the quasiclassical theory, we adapted the boundary conditions suggested in<sup>23</sup>. For numerical calculations the choice of a discrete grid of directions  $\mathbf{p}_F$  is of particular importance; we have shown how this grid must be chosen in order to guarantee current conservation perpendicular to the interface for an arbitrary scattering matrix. Thereafter we proposed a phenomenological random scattering matrix in order to describe microscopically rough interfaces without regular structure.

In section III we applied our model to mirror junctions and  $45^\circ$  asymmetric junctions with interface roughness. At first we studied the evolution of the temperature-dependent critical current for mirror junctions when increasing the interface roughness: We found that the non-monotonic behavior for a specular interface turns to a monotonic temperature dependence for rough interfaces. Therefore interface roughness is a possible explanation for the experimental results.

For the asymmetric junction we calculated the average current-phase relation, which describes large contacts ( $A \gg \xi_0^2$ ). We find a leading  $\sin(2\varphi)$ -like behavior of the current phase relation. This is in agreement with experimental findings<sup>12</sup> as discussed in Sec. III B. On the other hand we also showed that in small enough junctions

a dominating  $\sin \varphi$ -like contribution might be present. It would be interesting to check this effect experimentally.

In conclusion our results explain several aspects of the experimental data. In order to improve the theoretical description, a detailed description of the interface is necessary in the first place. For example facets, or a modified electronic structure near the interface, should be taken into account in a more realistic theory<sup>32</sup>.

## Acknowledgments

We would like to thank J. Mannhart and M. Ozana for stimulating discussions. This work was supported in part by the German Research Foundation (DFG).

- 
- \* Electronic address: lueckt@physik.uni-augsburg.de  
<sup>†</sup> A. F. Ioffe Physico-Technical Institute, 19021 St. Petersburg, Russia
- <sup>1</sup> D. A. Wollman, D. J. van Harlingen, W. C. Lee, D. M. Ginsberg, and A. J. Leggett, Phys. Rev. Lett. **71**, 2134 (1993).
  - <sup>2</sup> C. C. Tsuei, J. R. Kirtley, C. C. Chi, L. S. Yu-Jahnes, A. Gupta, T. Shaw, J. Z. Sun, and M. B. Ketchen, Phys. Rev. Lett. **73**, 593 (1994).
  - <sup>3</sup> Y. Tanaka and S. Kashiwaya, Phys. Rev. B **56**, 892 (1997).
  - <sup>4</sup> S. Kashiwaya and Y. Tanaka, Rep. Prog. Phys. **63**, 1641 (2000).
  - <sup>5</sup> T. Löfwander, V. S. Shumeiko, and G. Wendin, Supercond. Sci. Technol. **14**, R53 (2001).
  - <sup>6</sup> Y. S. Barash, H. Burkhardt, and D. Rainer, Phys. Rev. Lett. **77**, 4070 (1996).
  - <sup>7</sup> Y. Tanaka and S. Kashiwaya, Phys. Rev. B **53**, R11957 (1996).
  - <sup>8</sup> D. Dimos, P. Chaudhari, and J. Mannhart, Phys. Rev. B **41**, 4048 (1990).
  - <sup>9</sup> H. Hilgenkamp and J. Mannhart, Appl. Phys. Lett. **73**, 265 (1998).
  - <sup>10</sup> H. Arie, K. Yasuda, H. Kobayashi, I. Iguchi, Y. Tanaka, and S. Kashiwaya, Phys. Rev. B **62**, 11864 (2000).
  - <sup>11</sup> E. Il'ichev, V. Zakosarenko, R. P. J. IJsselsteijn, V. Schultze, H.-G. Meyer, H. E. Hoenig, H. Hilgenkamp, and J. Mannhart, Phys. Rev. Lett. **81**, 894 (1998).
  - <sup>12</sup> E. Il'ichev, V. Zakosarenko, R. P. J. IJsselsteijn, H. E. Hoenig, V. Schultze, H.-G. Meyer, M. Grajcar, and R. Hlubina, Phys. Rev. B **60**, 3096 (1999).
  - <sup>13</sup> E. Il'ichev, M. Grajcar, R. Hlubina, R. P. J. IJsselsteijn, H. E. Hoenig, H.-G. Meyer, A. Golubov, M. H. S. Amin, A. M. Zagorskin, A. N. Omelyanchouk, et al., Phys. Rev. Lett. **86**, 5369 (2001).
  - <sup>14</sup> B. Mayer, L. Alff, T. Träuble, R. Gross, P. Wagner, and H. Adrian, Appl. Phys. Lett. **63**, 996 (1993).
  - <sup>15</sup> J. Mannhart, H. Hilgenkamp, B. Mayer, C. Gerber, J. R. Kirtley, K. A. Moler, and M. Sigris, Phys. Rev. Lett. **77**, 2782 (1996).
  - <sup>16</sup> E. V. Thuneberg, M. Fogelström, and J. Kurkijärvi, Physica B **178**, 176 (1992).
  - <sup>17</sup> M. Fogelström, J. Sauls, and D. Rainer, Phys. Rev. Lett. **79**, 281 (1997).
  - <sup>18</sup> Y. S. Barash, A. A. Svidzinsky, and H. Burkhardt, Phys. Rev. B **55**, 15282 (1997).
  - <sup>19</sup> A. Poenicke, Y. S. Barash, C. Bruder, and V. Istyukov, Phys. Rev. B **59**, 7102 (1999).
  - <sup>20</sup> G. Eilenberger, Z. Phys. **214**, 195 (1968).
  - <sup>21</sup> J. Rammer and H. Smith, Rev. Mod. Phys. **58**, 323 (1986).
  - <sup>22</sup> A. Zaitsev, Sov. Phys. JETP **59**, 1015 (1984).
  - <sup>23</sup> A. Shelankov and M. Ozana, Phys. Rev. B **61**, 7077 (2000).
  - <sup>24</sup> K. Yamada, Y. Nagato, S. Higashitani, and K. Nagai, J. Phys. Soc. Jpn. **65**, 1540 (1996).
  - <sup>25</sup> T. Lück, U. Eckern, and A. Shelankov, Phys. Rev. B **63**, 64510 (2001).
  - <sup>26</sup> Y. Nagato, K. Nagai, and J. Hara, J. Low Temp. Phys. **93**, 33 (1993).
  - <sup>27</sup> N. Schopohl and K. Maki, Phys. Rev. B **52**, 490 (1995).
  - <sup>28</sup> A. Shelankov and M. Ozana, J. Low Temp. Phys. **124**, 223 (2001).
  - <sup>29</sup> C. Bruder, Phys. Rev. B **41**, 4017 (1990).
  - <sup>30</sup> M. Eschrig, Phys. Rev. B **61**, 9061 (2000).
  - <sup>31</sup> C. W. J. Beenakker, Rev. Mod. Phys. **69**, 731 (1997).
  - <sup>32</sup> J. Mannhart and H. Hilgenkamp, Rev. Mod. Phys. **74**, 485 (2002).
  - <sup>33</sup> R. Hopfengärtner, M. Leghissa, G. Kreiselmeier, B. Holzapfel, P. Schmitt, and G. Saemann-Ischenko, Phys. Rev. B **47**, 5992 (1993).
  - <sup>34</sup> H. Hilgenkamp, J. Mannhart, and B. Mayer, Phys. Rev. B **53**, 14586 (1996).
  - <sup>35</sup> L. B. Ioffe, V. B. Geshkenbein, M. V. Feigel'man, A. L. Fauchere, and G. Blatter, Nature **398**, 679 (1999).
  - <sup>36</sup> G. Blatter, V. B. Geshkenbein, and L. B. Ioffe, cond-mat/9912163.
  - <sup>37</sup> A. Huck, A. van Otterlo, and M. Sigris, Phys. Rev. B **56**, 14163 (1997).
  - <sup>38</sup> M. Fogelström and S.-K. Yip, Phys. Rev. B **57**, R14060 (1998).
  - <sup>39</sup> H. Burkhardt, Thesis, Universität Bayreuth (1997).
  - <sup>40</sup> M. H. S. Amin, A. N. Omelyanchouk, S. N. Rashkeev, M. Coury, and A. M. Zagorskin, Physica B **318**, 162 (2002).